J Solid State Eletrochem (2004) 8: 565–571
DOI 10.1007/s10008-004-0499-8

ORIGINAL PAPER

**Vadim B. Fetisov · Alexander N. Ermakov
Galina M. Belysheva · Andrey V. Fetisov
Valentin M. Kamyshov · Khiena Z. Brainina**

Electrochemical dissolution of magnetite in acid solutions

Received: 22 August 2003 / Accepted: 27 October 2003 / Published online: 5 March 2004

Abstract The present paper deals with the electrochemical behavior of magnetite microcrystals in an acid medium. A voltammetric method employing a carbon-paste electroactive electrode (CPEE) with an organic binder was used. It was found that the cathodic voltammograms, which were recorded at different scan rates, formed a set bounded in the space of i–E parameters by a ''generalizing'' voltammetric curve corresponding to the ''effective'' potential scan rate v_{eff}. In other words, all curves are situated under one enveloping curve, just as the smaller dolls sit in the largest doll of a ''Russian doll''. ''Reverse'' currents (a cathodic current in the anodic direction of the potential scan) were observed on the cyclic voltammogram. Forward and reverse currents obey the same laws and have one and the same ''generalizing'' curve, which could be taken as the magnetite characteristic.

Keywords Dissolution · Electrochemical reduction · Magnetite · Voltammetry

Introduction

The electrochemical reduction (dissolution) of magnetite in acid solutions has been dealt with in a number of studies (e.g. [1, 2, 3, 4, 5, 6, 7, 8, 9, 10]), which suggest that the reducing dissolution of Fe_3O_4 represents an irreversible process having a peaked response in the cathodic voltammogram (two [6, 11] or even three waves [2] of magnetite reduction are recorded when the potential scan interval is expanded). Therefore, the experimental results usually are interpreted using Vermilyea's relationship [12], which shows the decrease in the dissolution rate with growing overvoltage of both signs relative to the freely dissolving potential E_{fr} (without external applied potential). Strong objections have been voiced as to the applicability of Vermilyea's equation to ferrooxides [11, 13].

The decrease in the magnetite dissolution rate after the cathodic peak was explained in some studies by the appearance of a passivating film in the form of metallic iron [14], a donor–acceptor complex ($Fe^{III}O_2^-{}_{ads}$) [8], a continuous layer of adsorbed $H^+{}_{ads}$ hydrogen ions [3] or Fe^{2+} ions [9] on the electrode. The peaked dependence of the dissolution rate on the potential for Fe_3O_4 calls for further theoretical explanation [13].

The objective of the present study was to obtain more information about the electrochemical behavior of magnetite as an example of oxides having the spinel structure. This example was chosen because of magnetite is the main component for the synthesis of a wide class of magnetic oxides. The technique of voltammetry and a carbon electrode containing the solid substance to be investigated was used [15, 16].

Experimental

Materials

Magnetite samples were prepared by decomposing ferrous oxalate ($FeC_2O_4{\cdot}2H_2O$) of ''analytically pure'' grade in a flow of purified CO_2 by the following scheme: holding at 473 K, annealing at 873 K for 4–6 h, then cooling in a furnace in the same atmosphere. The Fe_3O_4 powder consists of particles with the average dimension $d_{av} = 14$ μm. The X-ray diffraction analysis of the samples was performed by the Debye–Scherrer method using Cr-K_α radiation on a DRON-3 diffractometer. According to the X-ray diffraction analysis, the samples contained one phase with the crystal lattice constant equal to 8.396 ± 0.0005 Å. This value agreed with the literature data for stoichiometric magnetite [17].

The experiments were performed using two batches of samples differing in their production time: the samples of batch A (A-magnetite) were synthesized more than two years ago and were exposed to air throughout this period, while the samples of batch B (B-magnetite) comprised a freshly prepared magnetite.

V. B. Fetisov · A. N. Ermakov · G. M. Belysheva
A. V. Fetisov · V. M. Kamyshov · K. Z. Brainina (✉)
Ural State University of Economy, 8th March St. 62,
620219 Ekaterinburg, Russian Federation
E-mail: baz@usue.ru

Instruments and electrodes

The electrochemical measurements were made by the method of voltammetry using a carbon-paste electroactive electrode (CPEE). The test material was added to the CPEE in the amount of 0.05–0.2 g per 1 g of the carbon paste prepared from a spectrally pure graphite grade "C-2" with particles of 40 μm or smaller in size. The binder was dibutyl phthalate added in the amount of 0.3 mL per 1 g of the dry mixture. The CPEE was polarized using a PI-50-1.1 potentiostat. The measured signal was displayed on a PC monitor screen. A glassy carbon crucible served as the auxiliary electrode and the electrolyzer, while the reference electrode was a saturated Ag/AgCl electrode type EVL-1M1. Supporting electrolytes were prepared from "suprapure" and "chemically pure" reagents and tridistilled water. The potential scan rate in the potentiodynamic mode was preset between 0.5 and 500 mV/s. The measurements were performed at room temperature in the potential interval from −0.8 to +0.7 V, in which the carbon paste is electroinactive and does not generate signals.

Results and discussion

A specific feature of the electrochemical dissolution of magnetite is a peaked shape of the voltammogram (e.g. [2, 3, 4, 9, 10, 11, 13, 16]). It has not been unambiguously explained in theoretical terms [13]. It may be shown (Fig. 1) that a peaked voltammetric curve of the A-magnetite turns smoothly to a wavy curve as the scan rate is increased. The latter curve is more characteristic for maghemite (see curve 1, inset in Fig. 1). The rate at which the curve starts transforming depends on the acid concentration of the solution and tends to decrease as the solution acidity diminishes. For example, a peaked response is observed only at $v \leq 5$ mV/s in a 0.01 M HCl solution. Probably, surface layers of the magnetite powder are partially oxidized already at the stage of production. It is known that this effect is frequent in the production practice of ferritic particles by the ceramic method. The exposure of the surface of a magnetite-graphite electrode to an oxygen-containing atmosphere may also cause a deviation of the surface layer composition from the stoichiometry towards Fe_2O_3 [18]. An analogous effect of the oxidation of the surface layer of

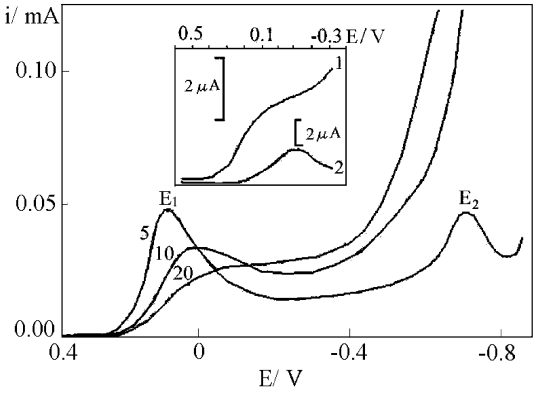

Fig. 1 Voltammograms of the A-magnetite (0.1 g/g) recorded at different potential scan rates in 0.5 M HCl. The *inset* has been adapted from [8]: *1*, γ-F_2O_3; *2*, F_3O_4

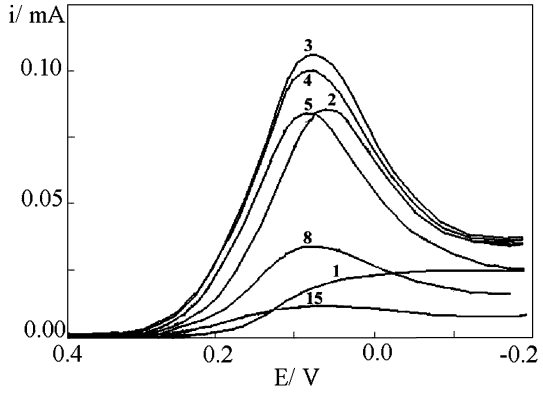

Fig. 2 Voltammogram of the A-magnetite (0.1 g/g) recorded during consecutive scans from a stationary potential (0.4 V) at a rate of 50 mV/s in 0.5 M HCl. The numbers on the curves denote the scan number

cadmium hexacyanoferrate was revealed recently [19]. The following observations also point to the presence of a higher oxide film on the surface of the magnetite particles. The peaked shape of the voltammogram characteristic for the magnetite (Fig. 2) is restored after repeated cathodic polarizations from the stationary potential. It is known [20] that the reaction depth (h) in an individual particle decreases with increasing scan rate. Therefore, one may expect that the number of consecutive scans, which need be realized to obtain the classical peaked shape, will grow correspondingly. For the case shown in Fig. 2, the electrode was polarized twice at a rate of 50 mV/s to remove completely the oxygen-enriched surface layer. The other assumption consists in that the decrease in current at $E < E_{fz}$ (potential of flat zones) is due to passivation processes, which are connected with appearance of a thin screening film on the surface of magnetite grains (see Introduction). The concepts mentioned are verified by chronoamperometric studies of two states of the A-magnetite, which differed in the presence (A_1 state) or the absence (A_2 state) of a thin film with superstoichiometric oxygen (relative to the volume of the sample) on the grain surface. The A_2 state was obtained by means of preliminary cathodic polarization of the magnetite electrode under dynamic conditions at the potential scan rate $v = 100$ mV/s. The chronoamperometric measurements were made in 6 M HCl at $E = -0.18$ V. It is known (e.g. [16, 21, 22]) that the oxidized form of the magnetite has a lower electrochemical activity than stoichiometric Fe_3O_4. Therefore, the A_1 magnetite may be viewed as a ready model demonstrating the effect of the coated film on the electrochemical dissolution of oxides. The surface limiting stage of the process usually shows up as a linear section in the "amount of interaction substance versus time" curve [23] or, which is the same, $i(\tau) = \text{const}$ as applied to chronoamperometric studies. From Fig. 3 it is seen that such a section is indeed present at the initial stage of the electrochemical dissolution of the A_1 magnetite (Fig. 3a). A similar chronoamperometric response

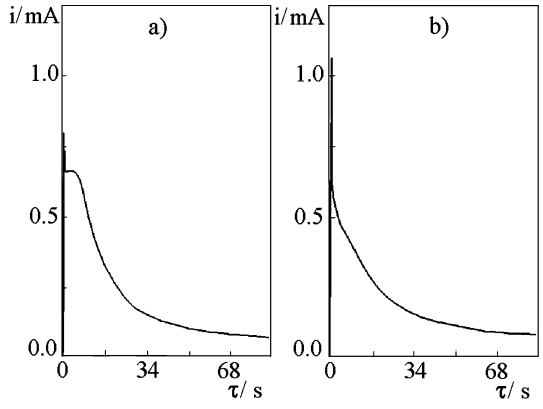

Fig. 3 Chronoamperograms of magnetite (0.2 g/g) recorded at $E=-0.180$ V in 6 M HCl: (**a**) the A_1 magnetite; (**b**) the A_2 magnetite

should also be expected for the A_2 magnetite if the cathodic polarization leads to replacement of the oxide film by a new passivating film [3, 8, 9]. Contrarily, over the whole time interval studied the kinetic curve for the A_2 magnetite (Fig. 3b) demonstrates the current drop as:

$$i \approx D^{-1/2}\tau^{-1/2} \quad (1)$$

pointing to a diffusion-controlled process.

Thus, the supposition about passivation processes during the cathodic polarization of the magnetite electrode was not confirmed in our experiments and the effect is due to the presence of a low electrochemically active oxide enriched by oxygen on the particles' surface.

Figure 4 presents a typical voltammogram of the A_1 magnetite in 0.5 M HCl solution registered at a potential between +0.4 and −0.9 V. When the potential scan rate is larger than 2 mV/s, the voltammogram exhibits two well-resolved peaks of the cathodic current at potentials of +0.2 to 0.0 V (E_1) and −0.70 to −0.80 V (E_2), depending on v. One more current maximum can be recorded if the potential scan interval is expanded in the cathodic direction [2].

The branches of the first peak obey the Batler–Volmer relationship. Their slopes depend on the potential scan rate. When the scan rate is smaller than some (let us call it "effective") potential scan rate v_{eff}, the slope of the

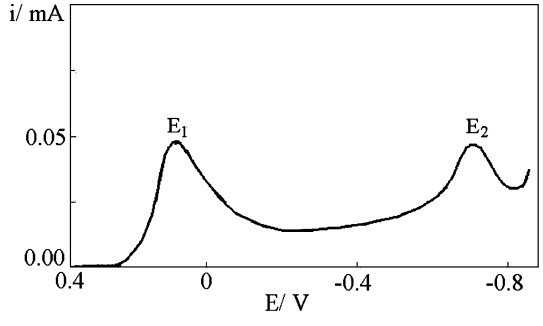

Fig. 4 Voltammogram of the A-magnetite (0.1 g/g) in 0.5 M HCl solution at $v=5$ mV/s

positive branch of the E versus log i curve is independent of v and equals 60 mV/unit. On the other hand, the slope of the negative branch strongly depends on v and changes from 125 to 280 mV/unit at 5 and 20 mV/s, respectively. At $v > v_{eff}$ a reverse phenomenon is observed, namely a strong dependence of the slope of the positive branch, which varies between 60 and 120 mV/unit, while the slope of the negative branch remains constant at a level of 280 mV/unit.

If the potential scan rate is increased, the peak potential shifts to the cathodic side. A rectilinear dependence of the peak potential on log$v$ probably has a general character. It was observed for materials of different origin (e.g. [18, 24, 25, 26, 27]). The function $I_m=f(v)$ in the case of the first peak (E_1) has an extremum (Fig. 5). When the scan rate is small, the ascending branch can be approximated by a linear dependence. As the acid concentration of the supporting electrolyte increases, the applicability boundary of the linear relationship shifts towards larger v.

The positive branch of the peak strongly depends on the acid concentration of the solution, while the negative branch is independent of pH. The potential E_1 versus the solution pH curve is linear and its slope increases from 140 to 200 mV/pH as v decreases from 5 to 1 mV/s, respectively. This fact probably suggests that protons are involved directly at the limiting stage of the process [11, 13, 18].

The second peak at E_2 behaves in accordance with the relationship $I_m \approx v^{1/2}$. An analogous behavior for the magnetite voltammograms was observed earlier [2, 18], with the only exception that in [2] the current near the peak (E_1) was independent of the potential scan rate.

Thus, the aforementioned results, which were obtained using a CPEE, agree fairly well with the literature data on the electrochemical dissolution of iron oxides. To avoid any surface oxide layer influence, freshly prepared B-magnetite was used for the subsequent experiments. This material produces a peaked response over

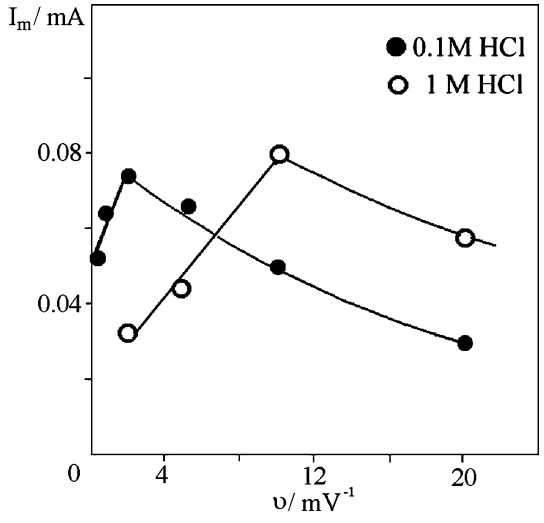

Fig. 5 I_m at E_1 versus potential scan rate (A-magnetite, 0.1 g/g)

the whole interval of the potential scan rates studied: from 0.5 to 500 mV/s.

Analysis of the experimental data concerning the effect of the scan rate on the magnetite dissolution voltammogram has shown that the set of recorded voltammograms has a certain pattern. The pattern character depends, in turn, on the structure of the surface layers of the crystals. It was mentioned in the foregoing that, unlike the aged A-magnetite, the freshly prepared B-magnetite produced a peaked response at all the scan rates studied up to 500 mV/s. This fact does not mean, however, that very thin layers with excess oxygen are absent on the B-magnetite surface. Therefore, a comparison experiment was performed. Electrochemical behavior of the initial B-magnetite samples (B_1) and samples from the same batch (B_2) were compared. The surface of grains in the latter samples was "cleaned" by preliminary cathodic polarization of the electrode from E_{st} to -0.2 V at a rate of 20–50 mV/s, depending on the acidity of the supporting solution. Some of the experimental results are shown in Fig. 6. From Fig. 6 it is seen that a generalizing polarization curve is present in both cases. This polarization curve outlines the region of permissible values of parameters in the "i versus E" space for the whole ensemble of voltammograms recorded at a preset acidity of the solution. In other words, the whole set of voltammograms fits the generalizing curve following a certain hierarchic principle depending on the sample preparation method (B_1 or B_2). When v is less or equal to v_{eff}, the ascending (positive) branches recorded for the B_1 and B_2 samples go along the positive branches of the generalizing i–E curves up to some value $J_m^{(i)}$, which depends directly on the scan rate. When $v > v_{eff}$, the ascending branches of the potentiodynamic curves recorded for the B_1 samples "break off" the generalizing peak and the descending branches merge together. $J_m^{(i)}$ decreases with increasing scan rate (Fig. 6a). A quick drop of the peak height with increasing v was also observed in [22].

When $v = v_{eff}$, the parameters of the voltammograms recorded for the B_2 samples flatten out and remain at a constant level over the whole range of the potential scan rates (see the inset in Fig. 6b).

When the solution acidity is higher than 1 M HCl, the B_1 samples partly deviate from the behavior described above: the voltammogram shifts towards more positive potentials at low scan rates and goes beyond the limits outlined by the generalizing curve. The potential scan rate at which the said deviation occurs depends on the acid concentration of the solution (2 and 5 mV/s in 2 and 4 M HCl, respectively). This exception to the rule provides an excellent support to the regularity we arrived at. When the HCl concentration of the solution is higher than 1 M, the set of voltammograms breaks up into two subsets. One of the subsets, which corresponds to larger v, fits the generalizing curve of the B_1 state (Fig. 6a). The other subset (with smaller scan rates) fits the generalizing curve of the B_2 state (see Fig. 6b).

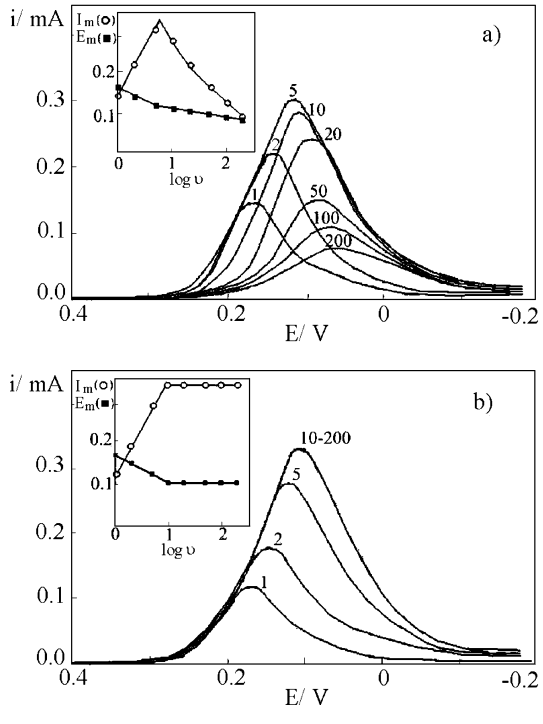

Fig. 6 Variation of the voltammograms of the B-magnetite (0.2 g/g) depending on the potential scan rate in 1 M HCl: (**a**) initial B_1 sample; (**b**) "cleaned" B_2 sample. The numbers on the curves denote the scan rate (mV/s)

Reverse currents

Anomalous phenomena in the form of a cathodic response during the polarization towards more positive potentials (the "reverse current" as defined in [28, 29]) were observed in studies concerned with the electrochemical dissolution of the magnetite under cycling conditions (e.g. [2, 3, 6, 7, 8, 9, 16]). Analogous effects, including those with the opposite sign (an anodic peak in the cathodic polarization curve), have been noted more than once in different systems on different electrodes (e.g. [28, 29, 30, 31, 32, 33, 34, 35, 36, 37]).

Figure 7 presents typical cyclic voltammograms of the B-magnetite, which were measured in a 0.5 M HCl solution using different scan rates from the stationary potential of 0.4 V to -0.2 V and back. It is seen that a well-defined cathodic peak appears at the polarization towards more positive potentials. All other things being equal, its value ($I_{m(rev)}$) depends, similarly to the value of the forward cathodic peak ($I_{m(fwd)}$), on the acidity and the temperature of the supporting electrolyte (a direct dependence), the concentrations of Fe_3O_4 and dibutyl phthalate in the paste (direct and inverse dependences respectively), and the potential scan rate (an extremum dependence for the A and B_1 states, flattening out for the B_2 magnetite). The reverse current is not detected when the scan rate is small and the electroactive species are exhausted on the electrode surface during the first half-cycle. The potential scan rate at which the reverse

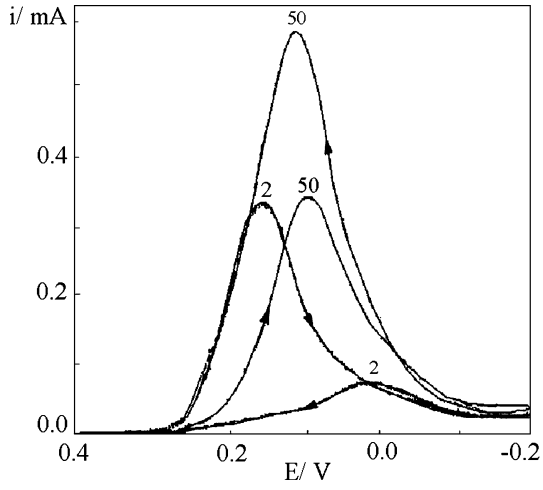

Fig. 7 Cyclic voltammograms of the B-magnetite (0.2 g/g) in 0.5 M HCl at potential scan rates equal to 2 mV/s and 50 mV/s

current is recorded directly depends on the HCl concentration of the solution. The anomalous current appears at $v > 5$ mV/s in a 1 M HCl solution and $v > 1$ mV/s in a 0.1 M HCl solution.

In a general case, the forward and reverse responses in cyclic voltammograms of the magnetite may differ considerably, both by their location on the potential axis and the intensity of the measured signals (Fig. 7). Remarkably, the potential values of the forward (E_{fwd}) and reverse (E_{rev}) peaks do not depend on their recording sequence. For example, cyclic voltammogram 1 in Fig. 8 was recorded when the potential was scanned at a rate of 2 mV/s in the cathodic direction from 0.4 V to −0.25 V and back. Curve 2 "started" at the same rate in the anodic direction from −0.25 V to 0.4 V and back. When the potential scan rate increases, the forward and reverse peaks approach one another both on the E axis and in their intensity until they merge completely at $v = v_{eff}$ (Fig. 9).

It should be noted that both sets of voltammograms fit one and the same generalizing curve. "Reversibility" of the shape of the magnetite cathodic response was observed earlier [2, 6, 9, 22]. The generalizing peak has a quite definite potential equal to ~0.1 V (Fig. 10) and,

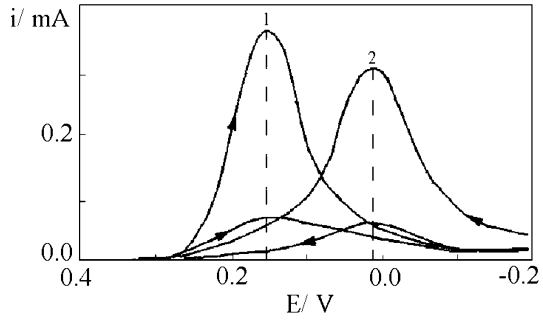

Fig. 8 Cyclic voltammograms of the B-magnetite (0.2 g/g) in 0.5 M HCl at a potential scan rate of 2 mV/s: *1*, from E_{st} to −0.25 V and back; *2*, from −0.25 V to E_{st} and back

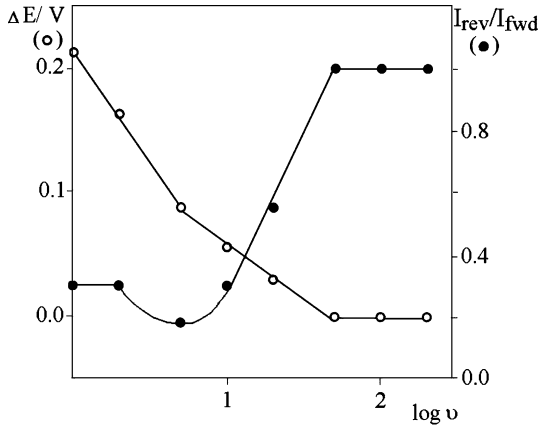

Fig. 9 Dependences of $\Delta E = E_{fwd} - E_{rev}$ and I_{rev}/I_{fwd} on the logarithm of the potential scan rate

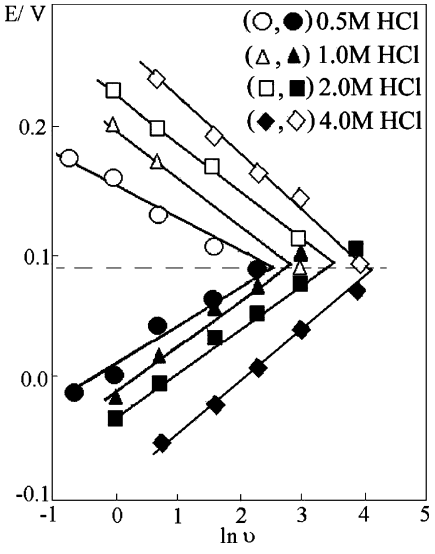

Fig. 10 Potentials of the forward (*open symbols*) and reverse (*filled symbols*) peaks versus the logarithm of the potential scan rate of the B-magnetite (0.2 g/g) at different HCl concentrations

therefore, this potential represents a characteristic of the magnetite.

The appearance of reverse currents in a cyclic voltammogram is often related to a unique origin of this effect, which is different from the origin of the forward signal in polarization curves. Sapozhnikova and Roizenblat [8] expressed this idea most clearly for a carbon paste electrode containing magnetite as the electroactive material. According to these authors, the current peak, which is recorded in the initial cathodic curve of the magnetite, is due to reduction of "nonstoichiometric" (as defined by the authors) trivalent iron $(Fe_B^{III}V'')^{\bullet}$ and is proportional to the concentration of vacancies in the lattice. The cathodic current in the anodic curve corresponds to reduction of iron bound to chemisorbed oxygen $[Fe^{III}O_2^-{}_{ads}]$ and depends on the concentration of bivalent iron in the magnetite. The analysis of our experimental data suggests that the forward and reverse

currents of the reducing dissolution of the magnetite obey the same laws and have one and the same generalizing curve. This may refute the assertion about a unique origin of the anomalous peaks.

In our opinion, at the polarization towards more positive potentials, when the reducing dissolution continues, the system passes the same sequence of states in the reverse direction as the forward (towards more negative) potential scan. Therefore, the material dissolves in the range of potentials where a region of homogeneity exists. In this case, the generalizing voltammetric curve reflects the change in the state of the material depending on the applied potential and essentially represents a voltammetric characteristic of the test material.

Conclusions

It was found that a kind of a "Russian doll" effect is realized for a carbon paste electrode containing magnetite as the electroactive material. The essence of this effect is that the whole set of voltammograms recorded at a given pH of the solution is bounded by a generalizing (as defined by us) curve corresponding to some "effective" scan rate $v_{\text{eff.}}$. The $v_{\text{eff.}}$ value is determined by the solution acidity.

It was shown that the change of the shape of the cathodic polarization curve with increasing potential scan rate and an extremum behavior of the $I_m = f(v)$ dependence (see Fig. 5) are indicative of an inhomogeneous structure of the magnetite particles (for example, a superstoichiometric concentration of oxygen in the surface zone of the crystals).

As concerning a "clean" surface of magnetite, the following supposition in all probability can be accepted. In the vicinity of the first peak (E_1) the reaction takes place in the homogeneity region of the defective structure of the magnetite according to the scheme:

$$Fe_{3\mp\delta}O_4 + 8H^+ + 2(1 \pm \delta)e^- \rightarrow (3 \mp \delta)Fe^{2+}_{aq} + 4H_2O \quad (2)$$

where δ is the potential-dependent parameter of nonstoichiometry. As the potential shifts towards more negative potentials, the defect content in the surface layer of the magnetite reaches a critical value ($+\delta_m$), which should be followed (analogously to the chemical reduction of nonstoichiometric oxides) by the crystal lattice failure. However, this process probably has insufficient energy near E_1. As a result of kinetic reasons, growth of the current on increase in the scan rate does not occur.

One may think that the electrochemical dissolution of the magnetite and the formation of the secondary solid phase take place over the region of potentials of the second peak (E_2). The formed FeO and Fe^{2+} dissolve in the electrolyte [38]. In all fairness, we have not had a direct indication to this course of the process yet.

An anomalous effect (a cathodic current in the potential scan towards more positive potentials) was observed during a cyclic polarization of the magnetite electrode. When the scan rate was equal to v_{eff}, the reverse cathodic response followed exactly the shape of the forward (cathodic) voltammetric curve of the magnetite (the shape reversibility). Obviously, the system reciprocates the sequence of states passed during the cathodic potential scan. In this case, a characteristic function of these states is the current strength $i(E)$, which reflects the electrochemical activity of a reagent depending on the applied potential.

Under certain experimental conditions ($v \geq v_{\text{eff}}$), CPEE voltammetric studies yield results similar to those obtained with compact disc electrodes. Correspondingly, the generalizing polarization curve may be used as a voltammetric characteristic of the magnetite.

References

1. Engell HJ (1956) Z Phys Chem 7:158
2. Haruyama S, Masamura K (1978) Corros Sci 18:263
3. Allen PD, Hampson NA, Bignold GJ (1980) J Electroanal Chem 111:223
4. White AF, Peterson ML, Hochella JrMF (1994) Geochim Cosmochim Acta 58:1859
5. Bruyere VJE, Blesa M (1985) J Electroanal Chem 182:141
6. Sukhotin AM, Gankin EA, Khentov AN (1975) Zaschita Metallov 11:165
7. Gorichev IG, Kipriyanov NA (1979) Zh Prikl Khim 52:473
8. Sapozhnikova EYa, Roizenblat EM (1974) Elektrokhimiya 10:1281
9. Lecuire J-M (1975) J Electroanal Chem 66:195
10. Lorenzo L, Encinas P, Tascon ML, Vazquez MD, de Francisco C, Sanches-Batanero P (1997) J Solid State Electrochem 1:232
11. Gorichev IG, Kipriyanov NA (1981) Zh Prikl Khim 11:2734
12. Vermilyea DA (1966) J Electrochem Soc 113:1067
13. Grygar T (1998) J Solid State Electrochem 2:127
14. Prazan M, Prazan V (1956) Czech Proc 21:73
15. Fiedler DA, Scholz F (2002) Electroanalytical methods. Springer-Verlag, Berlin Heidelberg, pp 211–222
16. Brainina Kh. Z, Neiman EYa (1993) Electroanalytical stripping methods. John Wiley & Sons, New York, pp 141–170
17. Glidewell C (1976) Inorg Chim Acta 19:45
18. Allen PD, Hampson NA, Bignold GJ (1979) J Electroanal Chem 99:299
19. Zakharchuk NF, Naumov N, Stösser R, Scholz F, Mechner H (1999) J Solid State Electrochem 3:264
20. Medvedeva EP, Rozhdestvenskaya ZB (1976) Vestnik Akad Nauk Kaz SSR 3:61
21. Encinas P, Lorenzo L, Tascon ML, Vazquez MD, Sanchez-Batanero P (1994) J Electroanal Chem 371:161
22. Lecuire J-M (1973) Analysis 2:489
23. Brown M, Dollimore D, Hallway A (1983) Solid-state reactions. Nauka, Moscow
24. Brainina KhZ, Lesunova RP (1974) Zh Anal Khim 29:1302
25. Grygar T (1996) J Electroanal Chem 405:117
26. Komorsky-Lovric S (1997) J Solid State Electrochem 1:94
27. Brainina KhZ, Vydrevich MB (1981) J Electroanal Chem 121:1
28. Brainina KhZ (1980) Elektrokhimia 16:678
29. Zakharchuk NF, Valisheva NA, Yudelevich JG (1980) J Anal Khim 35:1708
30. Brainina KhZ, Chernyshova AV, Stozhko NYu (1980) Elektrokhimia 16:1874
31. Brainina KhZ, Ashpur VV, Sokolov MA (1981) Elektrokhimia 17:400

32. Abrarov OA, Bighelis VM (1976) Elektrokhimia 12:688
33. Sunderland JG (1976) J Electroanal Chem 71:341
34. Noel M, Santhanam R, Chidambaram T (1998) J Solid State Electrochem 1:232
35. Jagner D, Sahlin E, Renman L (1996) Anal Chem 68:1616
36. Zakharchuk NF, Brainina KhZ (1998) J Electroanal Chem 10:379
37. Nolan MA, Kounaves SP (2000) Electroanalysis 12:96
38. Mutombo P, Hackerman N (1997) J Solid State Electrochem 1:194